

MODEL OF COMPOSITE DEGRADATION DUE TO ENVIRONMENTALLY ASSISTED FATIGUE DAMAGE

L N McCartney

NPL Materials Centre
National Physical Laboratory
Teddington, Middlesex
United Kingdom, TW11 0LW

Abstract

This report describes an extension, to account for the effects of fatigue loading, of a model that is able to predict the time-dependent axial residual strength of a unidirectional fibre reinforced composite arising from environmental exposure. The model assumes that environmental exposure leads to interfaces that are very weak so that a parallel two bar model can be developed where one bar represents the behaviour of the fibres which are regarded as a loose bundle, and where the second bar represents the matrix. The principal effect of the environment is assumed to be its effect on the time dependent strength of individual fibres arising from stress corrosion cracking of small defects within the fibres when the composite is subject to fatigue loading. The initial strength of the fibres is assumed to be governed by the Weibull distribution which, when used in conjunction with fracture mechanics, defines an initial statistical size distribution of fibre defects. Defect growth arising from environmentally assisted fatigue loading is assumed to be governed by a fracture mechanics based growth law where the defect growth rate is controlled by the stress intensity factor. The model has been extended to the case of cross-ply laminates.

The model developed for the prediction of the degradation of a unidirectional composite arising from stress corrosion cracking in the fibres under general time dependent loading is not suitable for application to high frequency fatigue loading. For the case of uniform amplitude fatigue loading the model can, however, be used to develop a very convenient method of predicting composite degradation. The methodology applies a factor Φ (≤ 1) to the time variable in order that degradation data for fixed applied loads can be used to predict degradation during uniform amplitude fatigue loading. The value of the factor Φ depends on the fatigue R-ratio, an exponent n appearing in the defect growth law, and on the nature of the fatigue cycle where sinusoidal and saw-tooth cycles (with dwell periods at maximum and/or minimum load) have been considered.

As the use of the factor Φ in conjunction with degradation data for the special case of fixed loading avoids having to consider fatigue loading, the methodology described once validated has potential for assessing the degradation of unidirectional composites without having to conduct difficult time-consuming and fatigue expensive tests. In addition, it is clear that static fatigue tests could be the basis of a method of accelerating dynamic fatigue tests. Model predictions indicate that there are good prospects for accelerating lifetime tests by carrying out tests at high loads (short lives) and then predicting long term behaviour using the linearity of the load vs $\log t_f$ measured relationship. The results of model predictions indicate that this could be the basis of a conservative approach to design.

© Crown copyright 2001
Reproduced by permission of Controller, HMSO

ISSN 1473-2734

National Physical Laboratory
Teddington, Middlesex, UK, TW11 0LW

No extracts from this report may be reproduced without the prior written consent of the Managing Director, National Physical Laboratory; the source must be acknowledged.

Approved on behalf of Managing Director, NPL, by Dr C Lea, Head of NPL Materials Centre

CONTENTS

Important notation	iv
1. Introduction	1
2. Model geometry	1
3. Basic mechanics for parallel bar model of composite.....	3
4. General time-dependent loading	4
4.1 Accounting for defect growth.....	5
4.2 Prediction of progressive damage	6
4.3 Predicting the failure stress and time to failure.....	8
4.4 Predicting residual strength	8
5. Environmentally assisted growth of damage during fatigue	10
6. Properties of the time factor.....	13
7. Extension of model to cross-ply laminates	15
8. Modelling effects of statistical variability.....	19
9. Accelerating fatigue testing	20
10. Conclusions	22
Acknowledgement	23
References	23

Important notation

A	Area of cross section of a single fibre
V_f	Fibre volume fraction
V_m	Matrix volume fraction
$F_b(t)$	Maximum load applied to the fibre bundle
$\sigma(t)$	Maximum stress in a surviving fibre
$\Delta\sigma(t)$	Stress range in a surviving fibre
$\sigma_b(t)$	Effective stress applied to the bundle of fibres
$\sigma_{app}(t)$	Effective stress applied to the composite
$\sigma_m(t)$	Maximum stress in the matrix
$\Delta\sigma_m(t)$	Stress range in the matrix
$\epsilon(t)$	Axial strain in fibres and matrix after time t
E_f	Young's modulus of the fibres
E_m	Young's modulus of the matrix
$E_b(t)$	Effective modulus of the fibre bundle
$E_c(t)$	Effective modulus of the composite
$N(t)$	Number of surviving fibres after time t
α	Dimensionless parameter defined by $V_m E_m / V_f E_f$
a	Parameter characterising fibre damage due to fatigue loading
$a_c(t)$	Critical value of a after time t
$X_o(t)$	Initial value of a that requires time t to reach the critical value $a_c(t)$
$\sigma_i(t)$	Initial strength of fibres that fail after time t
m	Weibull exponent
σ_o	Scaling stress used in Weibull distribution
$S(t)$	Residual strength after time t
A	Coefficient appearing in the fibre degradation law
n	Exponent appearing in the fibre degradation law
F	Maximum load applied during fatigue loading
F_{min}	Minimum load applied during fatigue loading
ΔF	Load range for uniform amplitude fatigue loading
R	Fatigue load ratio (F / F_{min})
ω	Frequency of uniform amplitude cyclic loading
Φ	Factor appearing in definition $\tau = t\Phi$ for 'reduced' time
\hat{x}	Normalised value of any quantity x
E_{90}	Transverse Young's modulus of the 90° plies
h_0	Total thickness of 0° plies
h_{90}	Total thickness of 90° plies

1. Introduction

The axial strength of unidirectional fibre reinforced composites is controlled by the strength of the fibres. In cross-ply laminates the axial strength of the laminate is controlled to a large degree by the strength of the fibres in the 0° plies. Fibre strength is statistical in nature due to the presence of defects both on fibre surfaces, and in their interior. This aspect has been described in an earlier report [1] that described a model of the environmental degradation of unidirectional composites subject to fixed axial loads. The effect of interface properties on axial strength are of secondary importance, and modelling their effect on axial strength requires the use of sophisticated stress transfer models and Monte Carlo simulation techniques; topics that have been considered in references [2, 3]. For unprotected glass fibres, it is well known (see for example [4]) that the environmental exposure of the composite leads to time dependent reductions in fibre strength. The strength reduction of the fibres results because of chemical effects (such as leaching) that affect the fibre properties, and because of the progressive growth of fibre defects caused by stress corrosion cracking at a microscopic level. Property degradation due to chemical effects has not been considered due to the significant technical difficulties of quantifying their effect in models, and of obtaining appropriate data to be used by such models. This aspect is an important phenomenon whose investigation is beyond the scope of the study.

Environmental exposure, for times long enough to reach saturation, can lead to a deterioration in interface properties. Given that the axial strength of a unidirectional composite is not affected to a great extent by interface properties, it is reasonable to assume, when modelling the effects of aggressive environments on the axial behaviour of unidirectional composites and cross-ply laminates, that the interfaces in the composite following prolonged exposure have no 'strength'. Because of the approximations that have to be made, the approach leads at best to a first order model. This enables a relatively simple approach to be taken that will provide good insight into the axial behaviour of a composite when exposed to both an aggressive environment and time dependent loading such as cyclic fatigue.

One objective of this report is to extend the existing model [1], that is valid only for fixed axial loads, so that the load carrying capacity of the matrix is taken into account when considering the axial behaviour of glass fibre reinforced composites subject to environmental exposure in the presence of time dependent loads, e.g. fatigue loading. A second objective is to use the model developed as the basis for investigating how both static and dynamic fatigue tests might be accelerated so that long-term performance can be estimated from shorter term tests.

2. Model geometry

Consider a unidirectional fibre reinforced composite having a fibre volume fraction V_f and matrix volume fraction V_m such that $V_f + V_m = 1$. The composite has been wholly immersed in an aggressive environment for a sufficient time for the composite to be fully saturated, and so that the chemical degradation of fibre and matrix properties is complete. The application of an axial load, which might be time dependent, leads to the environmental growth of defects in the fibres; a phenomenon well known to afflict glass fibres [4].

Following the approach of [1], the interfaces between the fibres and matrix are regarded as being significantly weakened by the environment to the extent that it can be assumed that the

fibres and matrix behave independently in regions of the composite that are well away from the uniaxial loading mechanism where clamping effects become important. This assumption means that the composite can be modelled as a parallel bar model, as shown in Fig.1. The fibres in the composite are regarded as acting as a loose bundle forming one bar of the model. The matrix material in the composite is considered as being gathered together to form the other bar of the model that is regarded as homogeneous, i.e. the bar is solid. When a fibre fails the load it carried is shared between the surviving fibres in the bundle and the matrix in such a way that all surviving fibres and matrix experience the same axial strain increment. The fibres are assumed to have the same length so that throughout the progressive failure process the stress in each surviving fibre has the same value that will be time dependent. The composite is subject to a time dependent applied load $F(t)$ for all times $t > 0$, where $t = 0$ corresponds to the time when the load is first applied. Environmental defect growth in the fibres leads to progressive fibre failure until the bundle collapses. It is assumed that bundle collapse corresponds to the catastrophic failure of the composite, i.e. the matrix strength is insufficient to maintain the load when all the fibres have failed. The objective is to develop the parallel bar model of a composite so that it can predict the dependence of composite life t_f on the time dependent applied load $F(t)$, and the dependence of the residual strength $F^*(t)$ of the composite on elapsed time t from the instant of first loading.

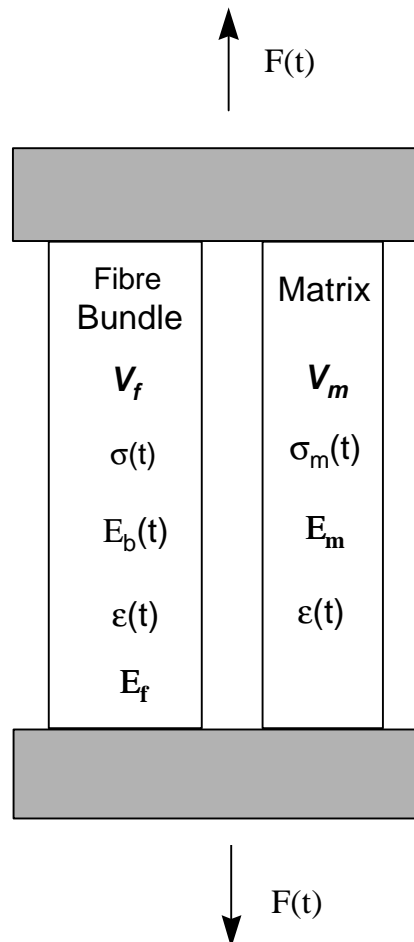


Fig.1 : Schematic diagram of the parallel bar model of a unidirectional composite that is used to predict the effects of environmental exposure on axial composite properties.

The behaviour of a unidirectional composite subject to environmental degradation has been modelled [1] for the case when the axial load applied to the composite is fixed in time. Thus the earlier modelling requires modification if it is to be applied to the prediction of the behaviour of a uniaxially loaded unidirectional composite material subject to time dependent loading, where cyclic loading is a case of great practical importance. Some of the relations given in this report have already been derived in [1], but are included here for the sake of completeness.

3. Basic mechanics for parallel bar model of composite

The analysis of the parallel bar model shown in Fig.1 neglects any axial thermal stresses arising from a mismatch of the thermal expansion coefficients of the fibres and the matrix. The area fraction of all fibres in the bundle is denoted by A_b , and that of the matrix is A_m . It follows that

$$V_f = \frac{A_b}{A_b + A_m} , \quad V_m = \frac{A_m}{A_b + A_m} = 1 - V_f . \quad (1)$$

The load applied to the fibre bundle element of the parallel bar model at time t is denoted by $F_b(t)$, the stress in each surviving fibre being denoted by $\sigma(t)$. The cross-sectional area of each of the fibres in the bundle is denoted by A , and the axial modulus of each fibre is denoted by E_f that is assumed to be time independent. The axial stress at time t in the matrix is denoted by $\sigma_m(t)$. The modulus of the matrix is denoted by E_m and is assumed to be independent of time. A time dependence could be included to account for visco-elastic effects, or for time-dependence arising from matrix ageing.

The axial strain in all surviving fibres of the bundle and the matrix has the same time dependent value that is denoted by $\varepsilon(t)$. As thermal expansion mismatch effects are neglected it follows that

$$\varepsilon(t) = \frac{\sigma(t)}{E_f} = \frac{\sigma_m(t)}{E_m} . \quad (2)$$

The balance of forces in the parallel bar model leads to the equilibrium relation

$$F_b(t) + A_m \sigma_m(t) = F(t) . \quad (3)$$

The number of surviving fibres in the bundle at time t is denoted by $N(t)$ so that the load applied to the bundle at time t may be written

$$F_b(t) = N(t)A\sigma(t) . \quad (4)$$

On substituting (4) into (3) followed by the elimination of $\sigma_m(t)$ using (2) it can be shown that the number of fibres surviving at time t is related to the fibre stress $\sigma(t)$ through the following relation quantitatively characterising the load sharing that occurs when fibres in the composite fail

$$\left[\frac{N(t)}{N_0} + \alpha \right] \sigma(t) = \frac{F(t)}{A_b}, \quad \text{where } \alpha = \frac{V_m E_m}{V_f E_f}, \quad (5)$$

and where $N_0 = N(0)$ and $A_b = N_0 A$.

It is useful to relate the number of fibres surviving in the bundle at time t to the effective axial modulus of the bundle $E_b(t)$. The effective stress applied to the bundle is defined by

$$\sigma_b(t) = \frac{F_b(t)}{A_b}. \quad (6)$$

Since the axial strain of the bundle and of the individual fibres has the value $\varepsilon(t)$ it follows that

$$\varepsilon(t) = \frac{\sigma(t)}{E_f} = \frac{\sigma_b(t)}{E_b(t)} = \frac{F_b(t)}{A_b E_b(t)} = \frac{N(t)}{N_0} \frac{\sigma(t)}{E_b(t)}, \quad (7)$$

where use has been made of (4) and (6). Clearly the effective axial modulus of the fibre bundle is given by

$$E_b(t) = \frac{N(t)}{N_0} E_f. \quad (8)$$

The effective stress $\sigma_{app}(t)$ applied to the composite at time t is defined by

$$\sigma_{app}(t) = \frac{F(t)}{A_b + A_m}. \quad (9)$$

It can be shown from (1) and (5), together with the fact that $A_b = N_0 A$, that

$$\sigma_{app}(t) = E_c(t) \varepsilon(t), \quad \text{where } E_c(t) = V_f E_b(t) + V_m E_m, \quad (10)$$

and where $E_c(t)$ is the effective axial modulus of the composite defined by the rule of mixtures, as to be expected.

4. General time-dependent loading

The objective here is to show how the earlier analysis [1], developed for fixed applied loads, must be modified for application to a unidirectional composite subject to time dependent loading such as that arising during fatigue loading. The analysis is based on the assumption that the strength of individual fibres is determined by surface defects whose effective size and distribution along the fibre surface is statistically distributed.

4.1 Accounting for defect growth

Fibre failure is assumed to be governed by a Griffith type of failure criterion having the form

$$\boxed{K^2(t) \equiv y^2 \sigma^2(t) a(t) = K_{Ic}^2}, \quad (11)$$

where $K(t)$ is an effective stress intensity factor at time t for a fibre defect of effective size $a(t)$ subject to a fibre stress $\sigma(t)$, K_{Ic} is the effective fracture toughness of the fibre material, and where y is a dimensionless parameter designed to account for defect geometry. The aggressive environment leads to defect growth when the fibre is under time dependent load. Such defect growth is assumed to be governed by a growth rate law of the form

$$\boxed{\frac{da(t)}{dt} = \Lambda K^n(t)}, \quad (12)$$

where Λ and n are material constants.

When a load is applied to a unidirectional composite, exposed to an aggressive environment to the point of saturation and to fatigue loading, the fibre defects grow in size according to the growth law (12) eventually leading to fibre failure when the failure criterion (11) is satisfied. Thus fibres progressively fail and the load carried by failed fibres is, for the parallel bar model under discussion, transferred to the surviving fibres and matrix using the load sharing rule (5). It is useful to present here the relationship that determines the initial defect size $X_0(t)$ that requires a time t to grow to the critical size $a_c(t)$, at which the fibre stress is $\sigma(t)$, under the influence of a time dependent fibre stress history $\sigma(\tau)$; $0 < \tau < t$. The critical defect size at time t is predicted by (11) to be

$$a_c(t) = \left[\frac{K_{Ic}}{y\sigma(t)} \right]^2, \quad (13)$$

and it can be shown on integrating (12) between the limits $X_0(t)$ and $a_c(t)$ that the initial size of defect failing at time t is

$$X_0(t) = \frac{K_{Ic}^2}{y^2} \left[\sigma^{n-2}(t) + (n-2) \lambda \int_0^t \sigma^n(\tau) d\tau \right]^{\frac{2}{2-n}}, \quad (14)$$

where

$$\lambda = \frac{1}{2} \Lambda K_{Ic}^{n-2} y^2. \quad (15)$$

On using (11) it follows from (14) that the initial strength $\sigma_i(t)$ of the fibres, that fail at time t when their stress is $\sigma(t)$, is given by

$$\sigma_i(t) = \left[\sigma^{n-2}(t) + (n-2) \lambda \int_0^t \sigma^n(\tau) d\tau \right]^{\frac{1}{n-2}}. \quad (16)$$

The cross-sectional area of the sample of unidirectional composite is assumed to be large enough for there to be a very large number of fibres. It can then be assumed that the bundle of fibres used in the parallel bar model contains every possible fibre strength that can arise in the statistical distribution. It is assumed that the strength distribution of the fibres is given by the two parameter Weibull distribution [5] so that, for a large bundle of N_0 fibres, the expected number of fibres N surviving when the stress in each fibre is σ is given by

$$\boxed{N = N_0 \exp \left[- \left(\frac{\sigma}{\sigma_0} \right)^m \right]}, \quad (17)$$

where σ_0 is a scaling parameter that will depend on the length of the composite.

In the subsequent analysis, the length of the material sample being modelled is not identified explicitly. The length of the sample affects only the value of the scaling parameter σ_0 . Strictly speaking the scaling parameter is of the form $\sigma_0 = s_0 / L^{1/m}$, where s_0 is the value of the scaling parameter for unit length of fibre, and this must be taken into account when applying the model. If the fibre/matrix interfaces are regarded as being very weak then clearly the relevant length to be used when specifying the value of σ_0 is that of the test sample. If the interfaces have some strength then smaller lengths can be taken as one can consider the UD composite as a series of bundles each having the same length. Unfortunately, no recommendation can be given of the appropriate length to use. It could be as small as the stress transfer length associated with fibre breaks, which are of the order of a few fibre diameters, or significantly larger.

4.2 Prediction of progressive damage

At time t the fibres that survive in the composite are those whose initial strengths were greater than $\sigma_i(t)$ defined by (16). It then follows from (17) that the expected number of surviving fibres $N(t)$ at time t is given by

$$\frac{N(t)}{N_0} = \hat{N}(t) = \exp \left[- \left(\frac{\sigma_i(t)}{\sigma_0} \right)^m \right]. \quad (18)$$

On substituting (16) in (18)

$$\left(\ln \frac{1}{\hat{N}(t)} \right)^{\frac{n-2}{m}} = \hat{\sigma}^{n-2}(t) + (n-2)\eta \int_0^t \hat{\sigma}^n(\tau) d\tau, \quad (19)$$

where

$$\eta = \lambda \sigma_0^2 = \frac{1}{2} \Lambda K_{lc}^{n-2} y^2 \sigma_0^2, \quad (20)$$

and where the use of the load sharing rule (5) leads to

$$\hat{N}(t) = \frac{\hat{F}(t)}{\hat{\sigma}(t)} - \alpha, \quad \text{or} \quad \hat{\sigma}(t) = \frac{\hat{F}(t)}{\hat{N}(t) + \alpha}, \quad (21)$$

where

$$\hat{F}(t) = \frac{F(t)}{N_0 \sigma_0 A}, \quad \hat{\sigma}(t) = \frac{\sigma(t)}{\sigma_0}. \quad (22)$$

On differentiating (19) with respect to time t and making use of (21) it is possible to derive two forms of differential equation governing progressive fibre failure in the composite. The first expresses the resulting differential equation in terms of $\hat{N}(t)$ while the second is expressed in terms of $\hat{\sigma}(t)$, (see [1]). For the case of time dependent applied loads, the choice of $\hat{\sigma}(t)$ as the unknown function of the differential equation is not ideal as the time dependence of $\hat{\sigma}(t)$ will follow the time dependence of the applied load. For fatigue loading this would mean that very small time steps might be needed to obtain accurate solutions of the differential equation. This problem is avoided by selecting $\hat{N}(t)$ to be the unknown function of the differential equation. It can be shown from (19) and (21) that

$$\left[\hat{F}^{n-2}(t) - \frac{\{\hat{N}(t) + \alpha\}^{n-1}}{m\hat{N}(t)} \left(\ln \frac{1}{\hat{N}(t)} \right)^{\frac{n-m-2}{m}} \right] \frac{d\hat{N}(t)}{dt} = \left\{ \hat{N}(t) + \alpha \right\} \hat{F}^{n-3}(t) \left[\frac{d\hat{F}(t)}{dt} + \frac{\eta \hat{F}^3(t)}{\{\hat{N}(t) + \alpha\}^2} \right]. \quad (23)$$

This differential equation is solved by standard numerical techniques [6] subject to the initial condition

$$\hat{N}_0 = \hat{N}(0) = \frac{\hat{F}(0)}{s_0} - \alpha, \quad (24)$$

where s_0 is the solution of the transcendental equation

$$\hat{F}(0) = s_0 \left[\alpha + e^{-s_0^m} \right], \quad (25)$$

that must be solved numerically. The corresponding value for the time dependence of the fibre stress $\hat{\sigma}(t)$ is obtained using (21)₂.

As shown in [1], the static strength of the composite (i.e. the initial strength) is given by F_{\max} where

$$\frac{F_{\max}}{N_0 \sigma_0 A} = \max \left\{ s_0 \left[\alpha + e^{-s_0^m} \right] \right\}. \quad (26)$$

4.3 Predicting the failure stress and time to failure

The structure of the differential equation (23) is such that $d\hat{N}/dt \rightarrow -\infty$ when $\hat{N}(t) \rightarrow \hat{N}_f$, occurring at time t_f where

$$\hat{F}^{n-2} = \frac{[\hat{N}_f + \alpha]^{n-1}}{m\hat{N}_f} \left(\ln \frac{1}{\hat{N}_f} \right)^{\frac{n-m-2}{m}} . \quad (27)$$

The time to failure t_f can be predicted only by solving the differential equation (23) in the range $N_0 \leq \hat{N}(t) \leq \hat{N}_f$.

4.4 Predicting residual strength

A key requirement concerning the effects of environment on composite degradation is the prediction of the time dependence of the residual strength of a composite. This has already been considered for the case of a unidirectional composite subject to a fixed applied load [1]. The objective now is to extend the analysis so that the residual strength of a unidirectional composite subject to time dependent applied loads can be predicted. After an elapsed time t from the application of a load history $F(t)$, the load is instantaneously increased until the composite fails catastrophically. Just before the load is suddenly increased the stress in the surviving fibres has the value $s(t)$ and at any stage during the subsequent instantaneous load increase the value of the stress in the fibres is denoted by s . When the fibre stress has the value s the critical defect size has the following value specified by (13)

$$a_c^* = \left(\frac{K_{Ic}}{ys} \right)^2 . \quad (28)$$

It is necessary to calculate the original size X^* of the critical defect using (11) and (12). It can be shown that

$$\left(X^* \right)^{\frac{2-n}{2}} = \left(a_c^* \right)^{\frac{2-n}{2}} + \frac{1}{2} \Lambda (n-2) y^n \int_0^t \sigma^n(\tau) d\tau . \quad (29)$$

On using (11) the initial strength of the fibres that are about to fail at time t , when the fibre stress has the value s , is denoted by s_i and is given, on using (29), by the relation

$$\hat{s}_i^{n-2} = \hat{s}^{n-2} + (n-2) \eta \int_0^t \hat{\sigma}^n(\tau) d\tau , \quad (30)$$

where use has been made of (20) and where

$$\hat{s}_i = \frac{s_i}{\sigma_0} , \quad \hat{s} = \frac{s}{\sigma_0} . \quad (31)$$

On using (19) the relation (30) may be written in the form

$$\hat{\sigma}_i^{n-2} = \hat{\sigma}^{n-2} - k(t) , \quad (32)$$

where

$$k(t) = \hat{\sigma}^{n-2}(t) - \left[\ln \frac{\hat{\sigma}(t)}{\hat{F} - \alpha \hat{\sigma}(t)} \right]^{\frac{n-2}{m}} . \quad (33)$$

The load applied to the composite F_s , when the fibre stress has the value s , is obtained from (21) and (22) so that

$$\frac{F_s}{N_0 \sigma_0 A} = \hat{F}_s = \hat{\sigma} \left[\alpha + \hat{N}_s \right] , \quad (34)$$

where \hat{F}_s is the normalised applied load and where \hat{N}_s is the normalised number of surviving fibres when the load on the composite is such that the fibre stress has the value s . It follows from (18) that

$$\hat{N}_s = e^{-\hat{\sigma}_i^m} . \quad (35)$$

On substituting in (34) the following expression is derived for the normalised load applied to the composite during a residual strength test

$$\hat{F}_s = \hat{\sigma} \left[\alpha + e^{-\hat{\sigma}_i^m} \right] . \quad (36)$$

The residual strength $S(t)$ of the composite at time t is the maximum value of F_s when s is varied, or alternatively the maximum value of \hat{F}_s when $\hat{\sigma}$ is varied. Noting that $k(t)$ is independent of $\hat{\sigma}$, the maximum value of \hat{F}_s occurs when $\hat{\sigma}_i = x(t)$ which satisfies the transcendental equation

$$1 + \alpha e^{x^m(t)} = m x^m(t) \left(1 + \frac{k(t)}{x^{n-2}(t)} \right) . \quad (37)$$

On using (32) the stress $s_{\max}(t)$ in the surviving fibres just before the composite fails during a residual strength test is obtained from

$$\frac{\sigma_{\max}(t)}{\sigma_0} = \left[x^{n-2}(t) + k(t) \right]^{\frac{1}{n-2}} = \hat{\sigma}_{\max}(t) . \quad (38)$$

It then follows from (32) and (36) that the residual strength of the composite $S(t)$, at an elapsed time t from the instant of first loading, is obtained using

$$\boxed{\frac{S(t)}{\sigma_0} = \hat{\sigma}_{\max}(t) \left[\alpha + e^{-x^m(t)} \right] = \hat{S}(t) .} \quad (39)$$

5. Environmentally assisted growth of damage during fatigue

When the composite is subjected to high frequency cyclic loading, the problem of solving the differential equation (23) becomes very difficult as exceedingly small time steps would need to be taken. This would lead to unacceptably long computation times and an accumulation of rounding errors that could not be estimated. In an attempt to avoid this difficulty it is now assumed that the applied load history $F(t)$ has a special form that describes uniform amplitude fatigue loading. Let F and F_{\min} be respectively the maximum and minimum loads that are applied during a fatigue cycle resulting at time t in maximum and minimum fibre stresses of $\sigma(t)$ and $\sigma_{\min}(t)$ respectively. It is assumed that the first occurrence of the maximum load occurs at the instant $t = 0$ when the load is first applied. Fig.2 shows a schematic diagram of one example of the type of loading that is to be considered where the time scale is taken as ωt so that numerically its value is a measure of the number of load cycles N_c that have been executed (i.e. $N_c = \omega t$), where ω is the frequency of cyclic loading (i.e. the number of cycles per unit of time).

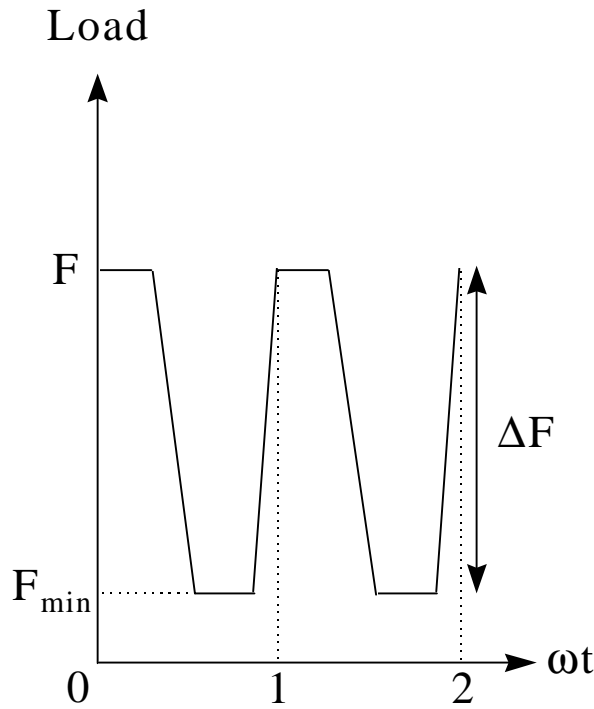


Fig.2 : Uniform amplitude fatigue loading with dwell periods at maximum and minimum loads.

The load range (i.e. amplitude) at any time t is assumed to be fixed at the value $\Delta F = F - F_{\min}$. The load history is assumed to be of the form

$$\frac{F(t)}{N_0 \sigma_0 A} \equiv \hat{F}(t) = \hat{F} - \Delta \hat{F} f(\omega t), \quad t \geq 0, \quad (40)$$

where

$$\hat{F} = \frac{F}{N_0 \sigma_0 A}, \quad \Delta \hat{F} = \frac{\Delta F}{N_0 \sigma_0 A}, \quad (41)$$

and where $f(\omega t)$ is a cyclic function of frequency ω such that its maximum and minimum values are 1 and 0 respectively, and such that $f(0) = 0$. For sinusoidal loading $f(x) = \frac{1}{2} \left\{ 1 + \sin\left(2\pi x - \frac{\pi}{2}\right) \right\}$. Other types of cyclic function can be defined to represent saw-tooth stress cycling, and stress cycles with dwell periods at maximum and/or minimum loads (see Fig.2).

The defect growth law is now considered over the time interval $t' \rightarrow t' + 1/\omega$ corresponding to the execution of one complete stress cycle. The time t' is assumed to correspond to a time at which the load has its maximum value. The approach is to assume that the fibre stress history $\sigma(t)$ is very nearly cyclic such that

$$\frac{\sigma(t)}{\sigma_0} \equiv \hat{\sigma}(t) = \hat{F}(t)\xi(t), \quad (42)$$

where the function $\xi(t)$ is expected to be slowly varying with time when compared to the time needed to execute just one fatigue cycle. The size of fibre defects, the number of surviving fibres and the maximum load are assumed to be slowly varying with time. The approach defined by (42) is justified by the load sharing rule (5) which shows that $\sigma(t)$ is proportional to $F(t)$ during a stress cycle provided that $N(t)$ is slowly varying on this time scale. It should be noted that when bundle failure is approached the function $N(t)$ is changing rapidly with time.

On using (11) to integrate (12) over the time interval needed to execute one stress cycle it can be shown that

$$a(t' + 1/\omega) - a(t') \equiv \frac{1}{\omega} \frac{da(t')}{dt'} \equiv \Lambda y^n \sigma_0^n \xi^n(t') a^{\frac{n}{2}}(t') \int_{t'}^{t'+1/\omega} \hat{F}^n(t) dt, \quad (43)$$

where the approximation assumes that the functions $\xi(t)$ and $a(t)$ are effectively time independent during the time interval of one stress cycle.

The relation (43) may then be expressed in the form of a fatigue crack growth law as follows

$$\frac{da(t')}{dt'} = \Lambda \Phi K(t')^n, \quad (44)$$

where the dimensionless parameter Φ is defined by

$$\Phi = \int_{\omega t'}^{\omega t'+1} \left(\frac{\hat{F}(t)}{\hat{F}} \right)^n d(\omega t). \quad (45)$$

It is emphasised that the result (45) for the time factor Φ will be invalid if the time per fatigue cycle becomes too long, as significant defect growth could occur during the stress cycle, especially as failure is approached.

The stress intensity factor is defined by (consistent with (11))

$$K(t') = y \sigma_0 \hat{F} \xi(t') a^{\frac{1}{2}}(t') = y \sigma(t') a^{\frac{1}{2}}(t') . \quad (46)$$

It should be noted from (40) that when $\Delta F = 0$ it follows from (45) that $\Phi = 1$ to the case of the application of a fixed applied load for all times $t \geq 0$.

It is clear that if a 'reduced' time $\tau = t' \Phi$ is introduced then the relations (44) and (46) may be written without loss of generality in the form

$$\frac{da(\tau)}{d\tau} = \Lambda K^n(\tau) , \quad (47)$$

$$K(\tau) = y \sigma(\tau) a^{\frac{1}{2}}(\tau) . \quad (48)$$

The result of taking account of uniform amplitude cyclic loading is merely to modify the value of the time with the result that the analysis and results given in [1] can be used directly for uniform amplitude fatigue loading provided that the time used in [1] is replaced by the value Φt , i.e.

$$t \int_{\omega t}^{\omega t+1} \left(\frac{\hat{F}(\tau)}{\hat{F}} \right)^n d(\omega \tau) . \quad (49)$$

There is no need to generate many new results in this report, as adequate predictions illustrating the capabilities of the model have already been made in [1]. The only useful additional information that will be provided here are estimates of the values of the parameter Φ for various types of uniform amplitude fatigue cycle. Before discussing this aspect it is first useful to relate the times of static loading to the number of cycles occurring when carrying out uniform amplitude fatigue loading.

When presenting the results of fatigue tests it is usual to plot the applied maximum stress of the fatigue cycle, normalised by dividing this stress by the static strength, as a function of the logarithm to base 10 of the number of uniform amplitude stress cycles. For uniform amplitude stress cycling at frequency ω the number of cycles executed at an elapsed time t is $N = \omega t$. For a static fatigue test carried out under a fixed load F , if the time to failure is t_f then, in the corresponding fatigue test having a maximum load F and stress range that leads to a value Φ for the time factor, the number of cycles to failure is given by $N_f = \Phi \omega t_f$. It thus follows that the S-N data should have the same shape as the static fatigue data. Also it follows that the waveform assumed for the cyclic loading case will not affect the shape of the S-N data. It will lead only to a shift along the cycles axis that will be at most one decade. This result is consistent with the conclusion of Sims & Gladman [7] who showed that triangular, sinusoidal and square waveforms had little influence on the shape of normalised S-N plot at large cycles to failure (>1000).

6. Properties of the time factor

It is useful to determine the value of the factor Φ for a range of types of uniform amplitude fatigue loading. The factor Φ depends on n the exponent in the defect growth law (12), and on the fatigue R-ratio that is defined by $R = F_{\min} / F$ where F_{\min} and F are the minimum and maximum loads applied during each fatigue cycle, as shown in Fig.2. Sinusoidal fatigue is a common type of uniform amplitude loading. Fig.3 shows the dependence of Φ on the R-ratio for the extreme values $n = 3$ and $n = 15$ for the exponent n in (12). It is seen that the value of the parameter n has a significant affect on the value of Φ for most values of the R-ratio. The value $R = 1$, for which $\Phi = 1$ and there is no effect of n , corresponds to the case of a fixed applied load (i.e. no stress cycling). A saw-tooth loading has also been considered such that the magnitude of the loading and unloading rates always has the same value. The dependence of Φ on R-ratio for this loading case is also shown in Fig.3. The value of Φ for sinusoidal loading is always greater than that predicted for saw-tooth loading. Also, the value of Φ is significantly less than unity for the smaller values of the R-ratio.

In Fig.4 the lines with circular and square symbols are values of Φ for the case when saw-tooth loading is used with the values $n = 3$ and $n = 15$ in conjunction with dwells periods which are included at either maximum or minimum load. The lines with diamond symbols shown in Fig.4 are the corresponding results (given in Fig.3) for the case when there are no dwell periods. The dotted and continuous lines denote predictions based on the values $n = 3$ and $n = 15$ respectively for the exponent in the fibre defect growth law (12). The values shown assume that the dwell period is one half of the cycle time, and that the magnitudes of the loading and unloading rates are identical. As to be expected the value of Φ for loading without dwells is always less than that for a dwell on maximum load, and always greater than that for a dwell on minimum load. It is worth noting that the value of Φ is affected significantly when $n = 15$ and there is also a dwell at minimum load. For the case where a dwell at maximum load is included in the load cycle, the reduction in the value of Φ is less marked.

In Fig.5, values of Φ are shown when $n = 3$ and 15 for loading cases where dwell periods are included at both maximum and minimum load. Each dwell has the same value and is taken to be one quarter of the cycle time, and again the magnitudes of the loading and unloading rates are identical. Fig.5 also shows the results given in Fig.4 for the case where dwell periods were included only at maximum load. Clearly the inclusion of the dwell period at minimum load has led to a reduction in the value of Φ at all values of the R-ratio.

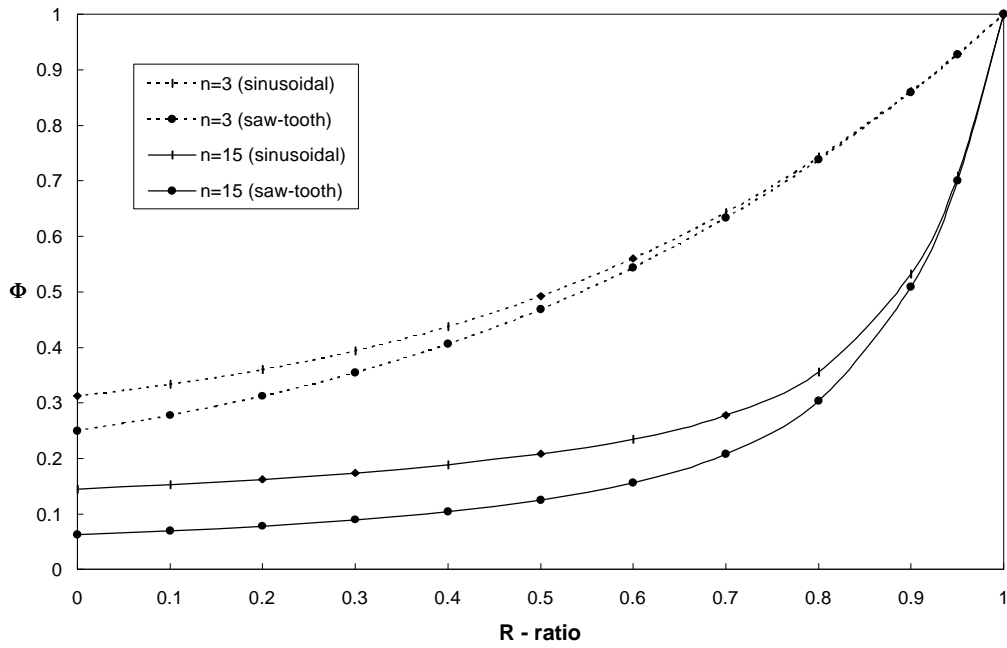


Fig.3 : The time factor F plotted as a function of the fatigue R-ratio without dwell periods.

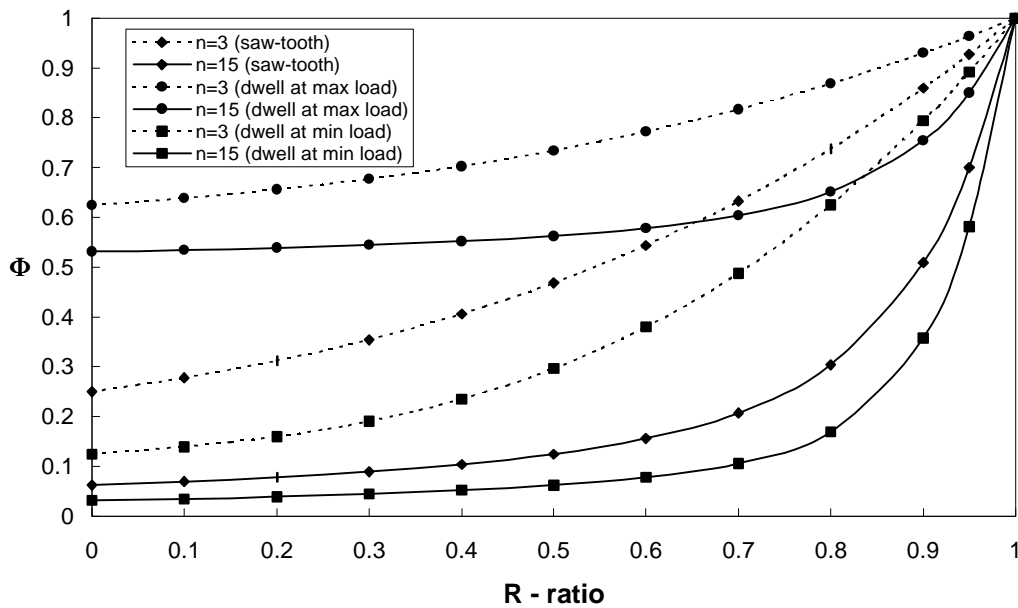


Fig.4 : The time factor F plotted as a function of the fatigue R-ratio with a single dwell period, either at maximum or minimum load.

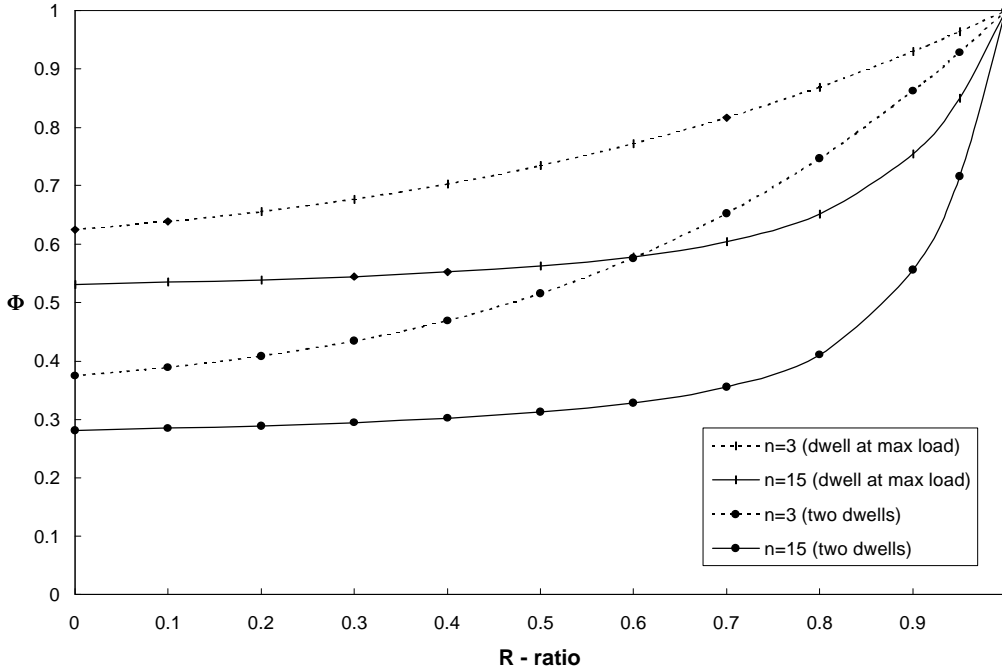


Fig.5 : The time factor F plotted as a function of the fatigue R -ratio with two dwell periods at maximum and minimum load.

7. Extension of model to cross-ply laminates

The next objective is to develop a model for cross-ply laminates that uses the same parallel-bar methodology that was used for unidirectional composites. The basic assumption is that all the plies in the cross-ply laminate may be separated and grouped together to form first of all two parallel bars. The first represents all of the 0° plies present in the laminate while the second represents all of the 90° plies. All the 0° plies are then broken up into a loose bundle of fibres and an additional bar representing the matrix of the 0° plies. The representative model is illustrated in Fig.6. It is assumed that the bar representing the 90° plies does not degrade and its properties are those of an undamaged ply for all stages of the degradation of the laminate. The axial Young's modulus for the 90° plies is denoted by E_{90} . In practice the 90° plies will degrade as a results of complex phenomena that are difficult to model, such as chemical effects that will modify properties. However, the mechanical effect of these plies on the failure of the laminate is of secondary importance and can be ignored when developing a first order model of laminate degradation.

The axial stress carried by the 90° plies at time t is denoted by $\sigma_{90}(t)$ and the total area of cross-section is denoted by A_{90} . The axial strain in all surviving fibres of the bundle of the 0° plies, the matrix of the 0° plies, and the 90° plies, has the same time dependent value that is denoted by $\varepsilon(t)$. As thermal expansion mismatch effects are neglected it follows that

$$\varepsilon(t) = \frac{\sigma(t)}{E_f} = \frac{\sigma_m(t)}{E_m} = \frac{\sigma_{90}(t)}{E_{90}} . \quad (50)$$

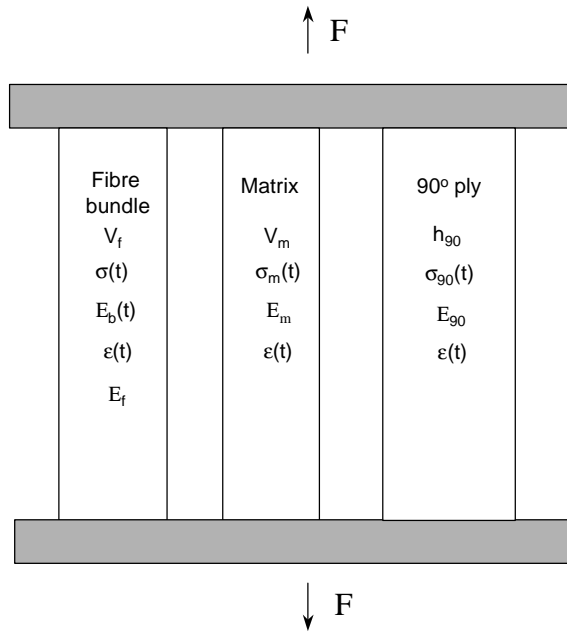


Fig.6 : Schematic diagram of the representation of a cross-ply laminate

The balance of forces in the parallel bar model leads to the equilibrium relation

$$F_b(t) + A_m \sigma_m(t) + A_{90} \sigma_{90}(t) = F(t) . \quad (51)$$

The number of surviving fibres in the bundle at time t is again denoted by $N(t)$ so that the load applied to the bundle at time t may be written

$$F_b(t) = N(t) A \sigma(t) . \quad (52)$$

On substituting (52) into (51) followed by the elimination of $\sigma_m(t)$ and $\sigma_{90}(t)$ using (50) it can be shown that the number of fibres surviving at time t is related to the fibre stress $\sigma(t)$ through the following relation that quantitatively characterises the load sharing that occurs when fibres in the composite fail

$$\left[\frac{N(t)}{N_0} + \alpha \right] \sigma(t) = \frac{F(t)}{A_b} , \quad \text{where } \alpha = \frac{V_m E_m}{V_f E_f} + \frac{h_{90}}{h_0} \frac{E_{90}}{V_f E_f} , \quad (53)$$

and where $N_0 = N(0)$ and $A_b = N_0 A$. The parameters h_0 and h_{90} are respectively the total thicknesses of the 0° and 90° plies. It is clear that the use of the parallel bar model to represent cross-ply laminates merely leads to a generalisation of the parameter α defined by (5)₂ for unidirectional laminates to the form defined by (53)₂.

It is useful to consider the values of the parameter α that arise when applied to a GRP that is susceptible to static and dynamic fatigue induced by stress corrosion mechanisms in the fibres. For a unidirectional E-glass fibre reinforced 913 epoxy composite having a fibre volume fraction of 0.51 (as measured [8] in the CPD2 Project), using the values $E_f = 72$ GPa

and $E_m = 3.39$ GPa in the relation (5)₂ that is valid for unidirectional composites leads to a value $\alpha = 0.0452$. For a $[0/90]_{4s}$ cross-ply laminate made of the same fibre and matrix materials, but having a fibre volume fraction of 0.565 (as measured in [8]), the relation (53)₂ for the cross-ply laminate leads to a much larger value of $\alpha = 0.381$.

The experimental results [8] obtained for unidirectional and cross-ply E-glass fibre/913 epoxy laminates are shown in Fig.7 where the normalised applied load is plotted as a function of the time to failure. It is seen that the cross-ply laminate degrades more rapidly than the UD composite but that both systems seem to tend to the same long time limit. It is now of interest to investigate the behaviour of the model.

In subsequent predictions it is assumed that the Weibull modulus for the initial strength distribution of the fibres is $m = 8$ and 1000 time integration points were used when solving the differential equation (23). There is some considerable uncertainty regarding the value of n that appears in the fibre defect growth law (12). The approach taken here is to consider first of all two extreme values of $n = 3$ and $n = 15$ in order to assess its effect on plots of the form shown in Fig.7 for experimental data. Fig.8 shows the comparison when using a value $\alpha = 0.1$ which is between the values $\alpha = 0.0452$ and $\alpha = 0.381$ relating to the UD and cross-ply materials used for experimental testing [8]. It should be noted that the results in Fig.8 are plotted as a function of ηt_f where η is defined by (20). This avoids having to specify values for parameters that are almost impossible to measure reliably, especially the parameter Λ appearing in the fibre defect growth law (12). Because $\log_{10}(\eta t_f) = \log_{10}(\eta) + \log_{10}(t_f)$ the predicted plots should correspond to the experimental data apart from a lateral shift that depends upon the value of η . In other words, if the experimental and predicted data are plotted on the same scale then the shape of the measured data and predictions should be the same if the model is accurately representing the measured data.

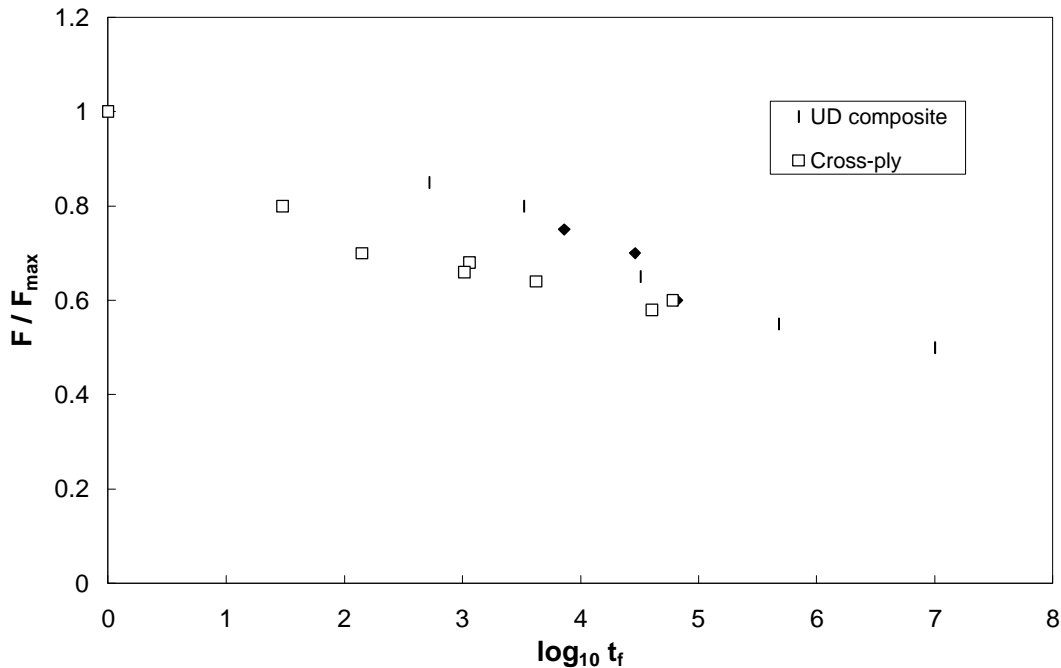


Fig.7 : Stress rupture of unconditioned unidirectional and cross-ply E-glass/913 in air.

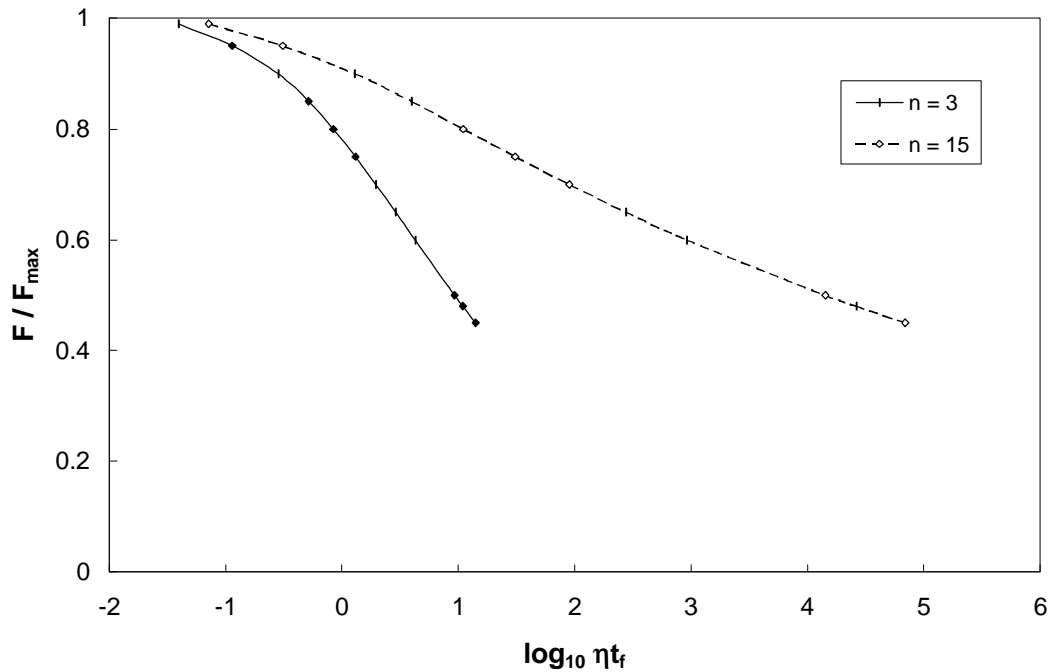


Fig.8 : Stress-failure time(normalised) plot of unidirectional composite when $m = 8$ and $a = 0.1$.

By comparing the experimental data in Fig.7 with the predictions in Fig.8 it is clear that the exponent $n = 15$ is much more representative of the measurements involving 6-7 decades on the time axis when compared with the predictions using $n = 3$ that only involves 3 decades on the time axis. It is in fact apparent that a larger value than $n = 15$ would lead to a better fit with the data. For this reason the value $n = 20$ is now selected.

Using values of α that are appropriate for the UD and cross-ply laminates given above to predict the stress-rupture behaviour of E-glass/913 epoxy laminates leads to the results given in Fig.9. It is clearly seen that the curves for the UD composite and the cross-ply laminate are almost identical so that the value of α used hardly affects results when plotted in the form of Fig.9. It is interesting to note that the experimental data given in Fig.7 are not inconsistent with this prediction of the model. The results for UD and cross-ply laminates shown in Fig.7 are seen to converge if the time to failure is large enough. For higher applied loads, leading to smaller times to failure, the UD composites are seen by experiment to degrade less rapidly than cross-ply laminates. While the model predicts the same trend, the difference in predicted behaviour is rather small when compared to the difference in the experimental results shown in Fig.7.

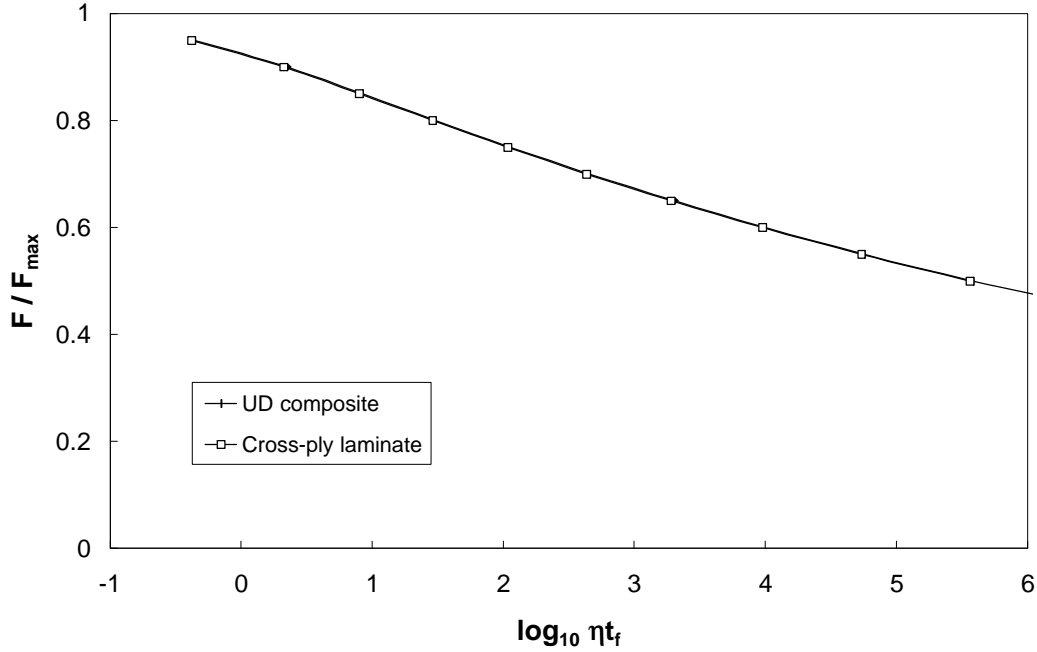


Fig.9 : Predictions of the stress-rupture behaviour of UD and cross-ply laminated E-glass/913 epoxy composites ($m = 8$, $n = 20$).

8. Modelling effects of statistical variability

It is emphasised that the model used to predict the results of Figs.8 and 9 is deterministic while the experimental data will be subject to scatter. It is useful to consider now the affect of both introducing scatter into the model, and replacing the weak interface model that has been the subject of this report by the model developed for stronger interfaces [9] that simulates statistical variability by including a Monte Carlo approach for the prediction of the behaviour of the 0° plies in a cross-ply laminate. It is assumed that the E-glass fibre volume fraction is 0.565, the fibre radius is 8 microns, and that thermal residual stresses are absent. The interfacial shear stress required by the model for strong interfaces is taken as 50 MPa, and the length of fibre/matrix element used in the Monte Carlo simulation is 1 mm. The fibre strength distribution is assumed to be characterised by a Weibull distribution having a Weibull modulus $m = 8$ and scaling factor 4.06 GPa. The exponent in the fibre defect growth law is taken as $n = 20$.

The first task is to estimate the expected initial strength of the laminate. By repeating the simulation of a static strength test five times, a reasonable estimate of average strength is obtained that is used to generate the normalised load F/F_{\max} that is plotted in Fig.10. On the time axis is plotted the dimensionless parameter ηt_f where η is the factor defined by (20). The factor η was not used when developing the model for strong interfaces, as an alternative scaling factor was introduced in the software [9]. In order that the predictions of the weak and strong interface models can be directly compared, it is necessary to apply a factor σ_0^2 / E_f^2 to the times generated by the strong interface model, as described in [9]. The result of comparing the predictions of the strong interface model described in [9] with the weak interface model that is the subject of this report is shown in Fig.10. It appears that both strong

and weak models predict the same type of curve, approximately linear with almost the same gradient. The strong interface model leads to longer lifetimes at all applied stress levels, although on a linear scale the difference in lifetime prediction can be up to a factor of 10. A major conclusion from this comparison is that the relatively simple weak interface model described in this report, that can be operated conveniently and quickly on PCs, leads to pessimistic predictions of lifetime, and could be considered as the basis of a design method. The more realistic strong interface model is more difficult to operate and it can take a considerable time performing simulations when the number of fibre/matrix cells used in the Monte Carlo simulation is large.

The other aspect to be considered is the degree of statistical scatter that arises when using the strong interface model. The results shown in Fig.10 indicate that there is some scatter in lifetime prediction, but that its magnitude is smaller than the predicted differences between the strong and weak interface models.

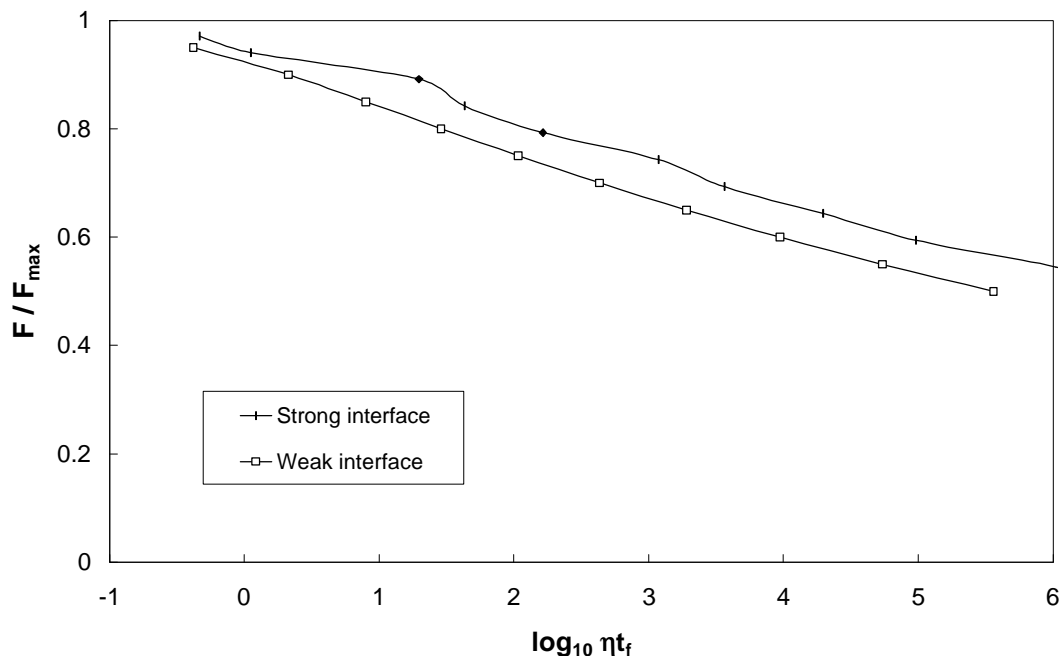


Fig.10 : Comparison of predictions of the stress rupture behaviour for strong and weak interface models applied to a GRP cross-ply laminate subject to uniaxial tension.

9. Accelerating fatigue testing

Both static fatigue and dynamic fatigue tests can require considerable time and effort that leads to cost penalties if the results of such tests are used in design procedures. There is, therefore, a strong motive to develop reliable methods of accelerating fatigue tests in order to reduce the costs of testing and data collection. Any reliable method will be based on a model (or models) that attempts to represent the degradation behaviour of composites in service conditions. The materials used for fibre and matrix cannot easily be varied in order to

accelerate testing, and neither can the environment in which the composite is to operate or be tested. While it might be possible to vary both material and environment in order to accelerate testing, it would require very sophisticated models that are capable of dealing with the chemical aspects of degradation. Models of composites having this capability, and of predicting damage growth and failure, do not yet exist. The only parameters at our disposal that can be used to accelerate testing are the loading parameters, the temperature and concentration of the environment (e.g. moisture), and perhaps the fibre volume fraction of the materials used. The approach taken here is to consider first how loading parameters might be used as a method of accelerating testing, as their effect is thought to be more dominant than temperature especially when chemical effects are not being modelled.

The model developed in this report is the basis of seeking a methodology to accelerate both static and dynamic fatigue tests. Consider first of all the case of dynamic fatigue tests for cases where stress corrosion cracking in fibres is the dominant damage and failure mode. It has been shown in Sections 3-6 of this report that the uniform amplitude fatigue performance of a unidirectional composite can be predicted from static fatigue tests by replacing the time t used in the static test by the time Φt that is relevant to dynamic fatigue tests. Since $\Phi \leq 1$ it is clear that any dynamic fatigue test will require a longer time to reach failure than for the equivalent static fatigue test. The corollary to this result is that if accelerated fatigue testing is desirable then, provided that the dominant damage mechanism is stress corrosion cracking of the fibres, it is recommended that large R-ratios are used if fatigue testing, but it would be better to perform static fatigue tests ($R=1$), followed by the application of the time factor Φ where the time t in the static fatigue test is replaced by t/Φ . Usually only modest acceleration factors will result, but if the exponent n is large then substantial acceleration factors are clearly attainable (i.e. up to a factor of ten when $n = 15$) as seen from the results in Fig.3. The results of comparing the data in Figs.7-9 does in fact indicate that $n = 15$ or $n = 20$ are more realistic values to use than $n = 3$ and this leads to more substantial acceleration factors.

The next question that arises is whether it is possible for static fatigue tests to be accelerated. The only method of achieving this is to perform tests at high loads so that failure times are relatively short, and then to apply a rule that enables the data collected to be extrapolated to the long lifetimes expected at low loads. The model developed in this report can be used for this type of investigation.

Fig.9 shows the result of using the model described in Sections 3-6 for the case of static loading to predict the dependence of the applied load ratio F/F_m on the normalised time to failure t_f . It is seen that for large enough times the plots are almost linear, and that this approximate linearity could be a basis for extrapolating data to longer lifetimes, perhaps one or two time decades longer. The issue of particular interest is how the gradient of these linear approximations are related to the parameters of the model. An examination of the analysis that was used to generate Fig.9, shows that the normalised time to failure is obtained from a complex differential equation (23) that will not yield an analytical result corresponding to a linear approximation. This is not really surprising as the curves in Fig.9 should tend to unity as $t_f \rightarrow 0$ and tend to zero as $t_f \rightarrow \infty$. Thus a linear approximation cannot be a good one to use across many decades of time, especially in view of the sigmoidal shapes of the curves that are just apparent in Fig.9. It is concluded, therefore, that the suggested linear extrapolation cannot easily be used to develop an accurate accelerated testing methodology for composite endurance. However, the extrapolation of the linear approximation will lead to reasonable

results if used over a limited number of time decades, and should lead to conservative estimates of times to failure if extrapolating over many decades. For the case of uniform amplitude fatigue loading, the time factor Φ can be applied to this linear interpolation method.

10. Conclusions

1. The model developed for the prediction of the degradation of a unidirectional composite arising from stress corrosion cracking in the fibres under general time dependent loading is not suitable for application to high frequency fatigue loading because of excessive computing times and the associated accumulation of rounding errors.
2. For the case of uniform amplitude fatigue loading the model can, however, be used to develop a very convenient method of predicting composite degradation. The methodology applies a factor Φ (≤ 1) to the time variable in order that degradation data for fixed applied loads can be used to predict degradation during uniform amplitude fatigue loading. The value of the factor Φ depends on the fatigue R-ratio, the exponent n appearing in the defect growth law (12), and on the nature of the fatigue cycle where sinusoidal and saw-tooth cycles (with dwell periods at maximum and/or minimum load) have been considered.
3. In principle, as the use of the factor Φ in conjunction with degradation data for the special case of fixed loading avoids having consider fatigue loading, the methodology described, once validated, has potential for assessing the degradation of unidirectional composites without having to conduct difficult time-consuming and expensive tests.
4. The weakly bonded model of lifetime and residual strength prediction can be extended from UD composites to the case of cross-ply laminates.
5. When comparing predictions of stress-rupture performance of the weak interface model with those of a strong interface model that requires Monte Carlo simulations, it is seen that the relatively simple and easy to use weak interface model leads to pessimistic predictions of lifetime. The weak interface model thus has some potential for use when developing new design methods for lifetime prediction.
6. An examination of the weak interface model, and its application to fatigue loading, has shown that there are some opportunities for accelerated testing that must be based on the model when interpreting measured data obtained from short term tests in a way that predicts long term behaviour. The modelling results indicate that any prediction of behaviour over long periods of time based on a linear extrapolation of lifetime data could be subject to a significant degree of uncertainty, but that the approach, leading to conservative estimates of lifetime, could be exploited in design.
7. While a modelling framework, that appears to be consistent with the trends of experimental results, has been established for the prediction of the effect of static and fatigue loading of unidirectional and laminated GRP composites subject to stress corrosion failure of the fibres, there remain significant gaps in capability that would have to be filled before a truly predictive methodology can be considered to have been established. One glaring lack in capability is the actual prediction of lifetime using time as the variable rather than the

dimensionless reduced time ηt which absorbs all the parameters needed by physical modelling that are very difficult, if not impossible, to measure directly. This is the major problem that confronts the development of physically based approaches to life prediction methodology, and a realistic assessment must conclude that it is highly unlikely that the problem will be solved on short timescales.

Acknowledgement

The report was prepared as part of the research undertaken for the Department of Trade and Industry funded project on 'Composites Performance and Design - Life Assessment and Prediction'.

References

1. McCartney, L.N., 'Model of composite degradation due to environmental damage', NPL Report CMMT(A)124, September 1998.
2. McCartney, L.N., 'Analytical model for debonded interfaces associated with fibre fractures or matrix cracks', in Proc. ICCM-12, Paris, July 1999.
3. McCartney, L.N., 'Simulation of progressive fibre failure during the tensile loading of unidirectional composites', NPL Report CMMT(A)212, August 1999.
4. Metcalfe, A.G., Gulden, M.E. and Schmitz, G.K., *Glass technology*, **12**, (1971), 15-23.
5. Weibull, W., 'A statistical distribution function of wide applicability', *Journal of Applied Mechanics*, **19**, (1951), 293-297.
6. Churchhouse, R.F., 'Handbook of Applicable Mathematics', Vol. 3 on 'Numerical Methods', series edited by W Ledermann, John Wiley and Sons, Chichester - New York - Brisbane - Toronto, 1981, pp. 319-321.
7. Sims, G.D. and Gladman, D.G., 'A framework for specifying the fatigue performance of glass fibre reinforced plastics', NPL Report DMA(A)59, Dec. 1982.
8. W.R.Broughton, M.J.Lodeiro & S.Maudgal, 'Accelerated test methods for assessing environmental degradation of composite laminates', NPL Report CMMT(A)251, November 2000.
9. L.N.McCartney, 'Simulation of progressive damage formation and failure during the loading of composites', NPL Report MATC(A)20, May 2001.

The theory in the report is used in software application BUNDLES\FATIGUE\PHI
The filename of the report is Papers\Env_Fatigue.doc